

4-26-2020

Metal Layer Architectures for 2D TMD Heterostructures

Anna K. Benton
University of Dayton

Follow this and additional works at: https://ecommons.udayton.edu/uhp_theses

eCommons Citation

Benton, Anna K., "Metal Layer Architectures for 2D TMD Heterostructures" (2020). *Honors Theses*. 248.
https://ecommons.udayton.edu/uhp_theses/248

This Honors Thesis is brought to you for free and open access by the University Honors Program at eCommons. It has been accepted for inclusion in Honors Theses by an authorized administrator of eCommons. For more information, please contact frice1@udayton.edu, mschlengen1@udayton.edu.

Metal Layer Architectures for 2D TMD Heterostructures



Honors Thesis

Anna K. Benton

Department: Chemical and Materials Engineering

Advisor: Christopher Muratore, Ph.D., Ohio Research Scholars

Endowed Chair

April 2020

Metal Layer Architectures for 2D TMD Heterostructures

Honors Thesis

Anna K. Benton

Department: Chemical and Materials Engineering

Advisor: Christopher Muratore, Ph.D., Ohio Research Scholars Endowed Chair

April 2020

Abstract

2-Dimensional transition metal dichalcogenides (TMDs) are of interest because of their potential for use in transistors and sensors due to their unique electronic and optical properties, coupled with mechanical flexibility. The band gaps of TMDs differ depending on the transition metal and dichalcogenide, the thickness of the TMD, and the structure of the TMD. To be able to tune the electronic and optical properties of TMDs, thin transition metal layers of molybdenum, tungsten, and rhenium were deposited on a silicon substrate with a 200nm oxide layer using a magnetron sputtering chamber. The film thickness and structure, surface characteristics, and conductivity were measured using atomic force microscopy, scanning electron microscopy, and a voltmeter, respectively. The thin transition metal films were then sent to collaborators to be exposed to sulfur or selenium to form TMDs. The TMD heterostructure will then be characterized using an AFM, SEM and Raman Spectroscopy. Then, transition metal bilayers were formed by sequentially depositing the transition metals on the silicon substrate with a 200nm oxide layer using a magnetron sputtering chamber. The film characteristics were then determined using the same methods as the single transition metal layer. The transition metal bilayers were then sent to collaborators to be exposed to sulfur or selenium to form TMDs. The bilayer TMD heterostructure will then be characterized using an AFM, SEM and Raman Spectroscopy and its optical and electronic properties will be characterized. Specifically, the electronic band gap will be evaluated and compared to the values for the monolithic monolayers. By varying the order of TMD layers, semiconductors with different band gaps will be able to be produced. This would allow for greater tailorability of the TMD semiconductors for use in applications such as flexible transistors and molecular sensors.

Acknowledgements

I would like to thank everyone that supported me in this endeavor; my UD mentor Dr. Christopher Muratore, my AFRL mentor Dr. Nick Glavin, the project collaborators Dr. Mike Snure (AFRL) and Dr. P. Ajayan (Rice University), the AFRL/UD research team, and my family and friends.



University of
Dayton

Table of Contents

Abstract	Title Page
Introduction	1
Equipment and Procedure	5
Results and Discussion	11
Conclusion and Recommendations	17
Future Work	18
References	19

Introduction

Two-dimensional (2D) transition metal dichalcogenides (TMDs) are semiconductors that are promising for many applications including transistors and sensors. A number of 2D TMDs have a direct band gap that allows them to conduct electricity when the band gap is surpassed. Tuning of the band gap to absorb or emit light at a given wavelength can be accomplished by stacking TMDs like Legos. Figure 1 displays how the monolayers of TMDs would interact using van der Waals interactions much like how Legos lock together (Geim & Grigorieva, 2013). By varying the stacking of the TMDs, a range of band gaps can be produced. This would allow for greater tailorability of the transistors and sensors and light harvesting devices using the stacked TMD heterostructures.

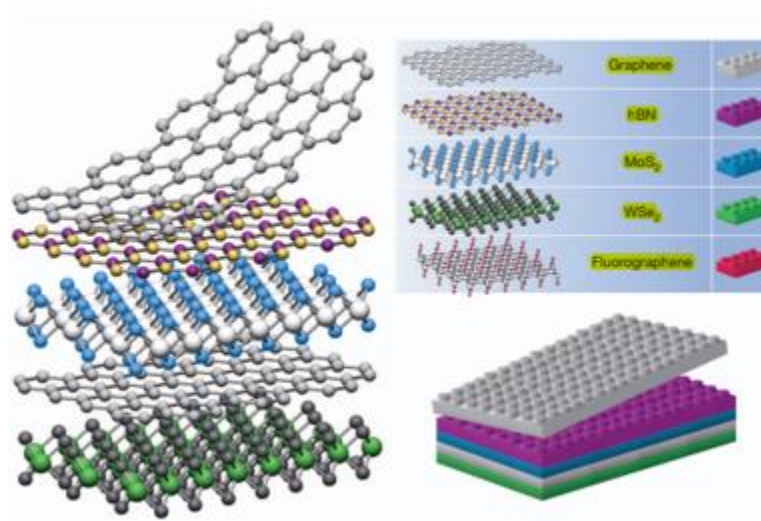


Figure 1: Stacks of Monolayers

One of the challenges with stacking the monolayers is growing continuous monolayer films. The weak van der Waals interactions favor growth of metal islands instead of growth of a continuous monolayer (Geim & Grigorieva, 2013). To overcome

this limitation, a transition metal film was deposited on a substrate in a magnetron sputtering system (Figure 2). Then, the metal film was exposed to a gaseous chalcogenide to form the TMD. Since the metal deposited on the substrate in a continuous layer, when the metal layer is exposed to the chalcogenide then the newly formed TMD should also be a continuous layer.

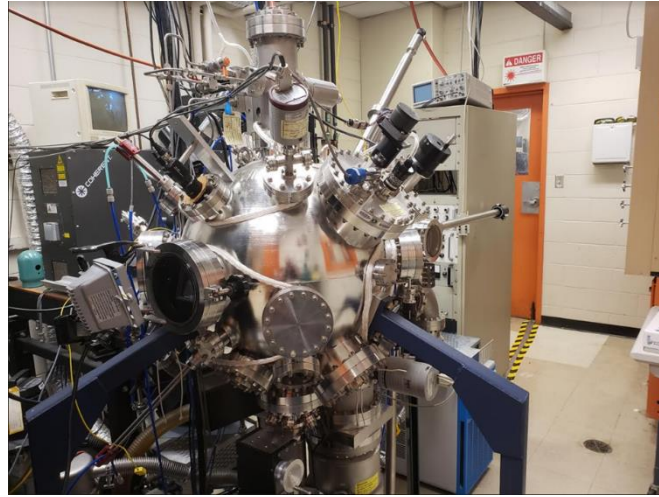


Figure 2: Physical Vapor Deposition Magnetron Sputtering System

There are a number of intrinsic processing conditions, such as the energy and density of incident atoms, that can cause a change in the morphology of the metal film. The best morphology for the application of interest will demonstrate minimal roughness and be uniform and continuous even though it is very thin ($<2\text{nm}$). Many samples were produced to determine which conditions yield the most conducive for stacking in terms of roughness and continuity over the surface. One way to change the film morphology is by varying the power density supplied to the sputtering target. Low power (direct current, DC) supplies a lower power density to the sputtering target and generally produces less dense deposited films. Medium power (pulsed direct current, PDC) supplies a similar, lower power density to the sputtering target like dc sputtering, but for a short period of

time a positive charge is applied to the sputtering target which significantly increases the kinetic energy of incident ions during film growth. This results in enhanced surface diffusion and produces denser films than expected from a dc supply. High power (High-power impulse magnetron sputtering, HiPIMs) supplies a high-power density to the sputtering target resulting in a highly ionized incident metal flux, significantly impacting the film structure and properties (Ehiasarian, et al., 2002). In addition to varying the charge density supplied by the power supply, the temperature of the substrate at deposition was varied because temperature can have an effect on the film morphology (Petrov, Barna, Hultman, & Greene, 2003). The two temperature conditions were room temperature (approximately 25 °C) and 500 °C. The thickness of TMD films can have a strong effect on their properties after exposed to gaseous sulfur/selenium, so many deposition times were produced in order to determine the limit on the thickness of films still demonstrating continuity across their surface (Jung, et al., 2014) (Dumceno, et al., 2015).

The last variation of growth was with the transition metal used for deposition. Each transition metal dichalcogenide has a unique band gap. In order to have the greatest tailorability, a wide spectrum of band gaps need to be able to be synthesized, which requires many different transition metal layers with a large range in band gaps. The metal deposition conditions that were repeated for each metal are listed in Table 1.

Table 1: Metal Deposition Conditions

Power Supply	Deposition Time (s)	Temperature (°C)	
		25	500
DC	2	25	500
DC	4	25	500
DC	6	25	500
DC	8	25	500
PDC	2	25	500
PDC	4	25	500

Power Supply	Deposition Time (s)	Temperature (°C)	
		25	500
PDC	6	25	500
PDC	8	25	500
HiPIMs	5	25	500
HiPIMs	10	25	500
HiPIMs	15	25	500
HiPIMs	20	25	500

Equipment and Procedure

Transition Metal Film Growth

A physical vapor deposition magnetron sputtering system was used to deposit the molybdenum, tungsten, and rhenium metal films (Figure 3). Silicon dioxide substrates, typically 1 cm x 1 cm square, were cleaned using methanol. The room temperature samples were attached to the substrate holder using vacuum safe carbon tape. The tape covered part of the substrate surface, masking a portion of the surface and allowing the thickness of the metal film to be determined after metal deposition. The 500 °C samples are not taped, because at the elevated temperature the carbon tape vaporizes, thereby contaminating the substrate. The substrate holders containing the substrates were then placed in the sample chamber.

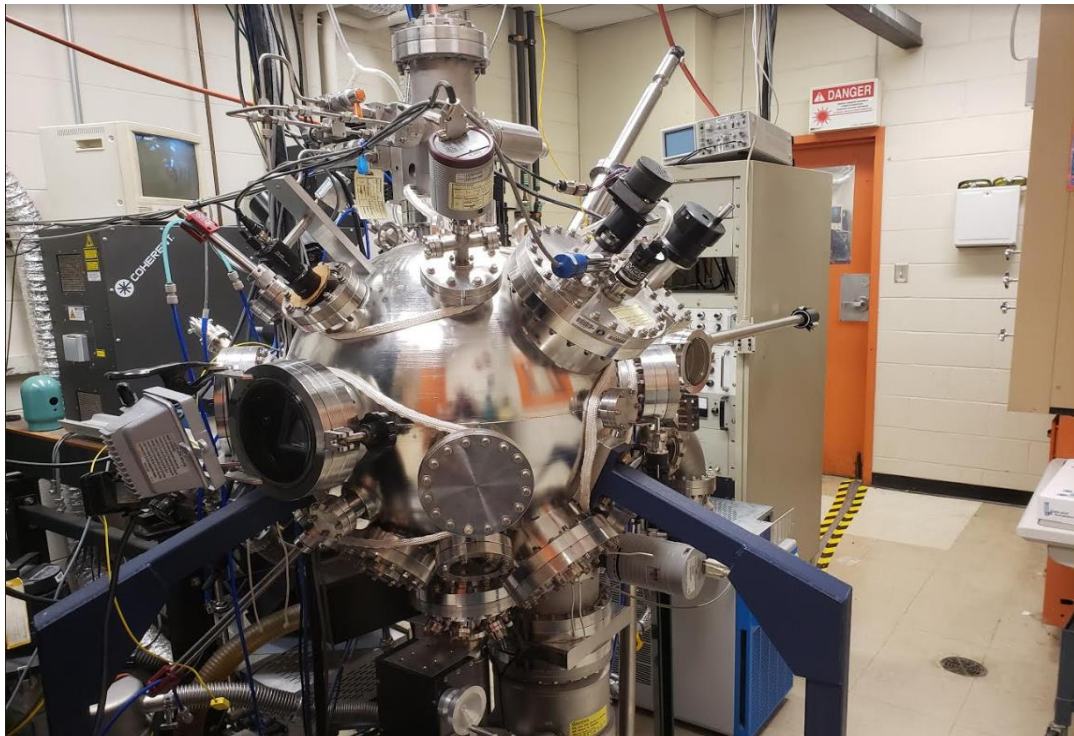


Figure 3: Physical Vapor Deposition Magnetron Sputtering System

Before deposition of a new material, the target was cleaned by sputtering its surface in the absence of a substrate. This ensures the desired target is not covered by another material and that the only vapor deposited on the substrate is of the desired composition. Both of these prevent contamination of the metal films. After the target is cleaned, the sample holder containing the substrate is placed in the deposition chamber. The sample is adjusted to the optimum height for exposure to the vapor using a movable sample stage. The sample is also rotated in the chamber during deposition to ensure film uniformity across the entire substrate.

Characterization of Transition Metal Films

After the metal films were deposited on the silicon dioxide substrates, the metal films were examined to determine which deposition conditions produced the desired film characteristics.

An atomic force microscope (AFM) was used to measure the thickness and the morphology of the metal film. The thickness was measured on room temperature samples by using the ridge produced by the carbon tape. An optical microscope image of the AFM probe tip on the edge between the metal film and the substrate is shown in Figure 4.

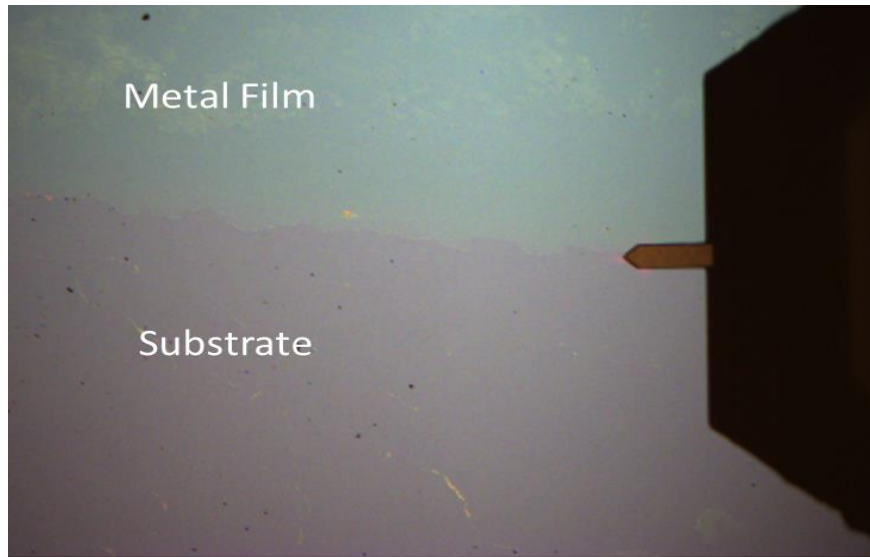


Figure 4: AFM probe tip on edge between metal film (blue) and substrate (pink)

The area scanned was $50\ \mu\text{m} \times 12.5\ \mu\text{m}$, with the long end perpendicular to film edge. This large area was scanned to reduce the edge effects and better represent the bulk film thickness. The step function of the program Nanoscope was used to determine the height. The step function takes the difference in height between two selected areas, in this case the metal film and the substrate. The thickness of $500\ ^\circ\text{C}$ samples was assumed to be comparable to room temperature depositions of the same deposition time, as there was no mask applied to their surfaces to create the ridge used for thickness measurement. The morphology of the films was measured on all samples away from any debris or edges to best represent the bulk film. Through trial and error, $500\ \text{nm} \times 125\ \text{nm}$ was determined to be the ideal area because multiple metal clusters could be scanned in detail. The root mean square (RMS) roughness was recorded for each film to determine how the relative roughness of the metal films changes with deposition conditions.

A scanning electron microscope (SEM) was used to identify surface morphology and characteristics of the metal films. Efforts to image the samples were generally

focused on the edge of the metal film and the substrate to see contrast and confirm continuity observed on the AFM. The metal cluster size was too small to be seen on the SEM, so only large-scale (scale order) film characteristics were observed. Few SEM images were taken on the metal samples due to the minimal additional information gained and limited time to complete the project.

A traditional electrical probing station was used as a direct indicator of film continuity (Figure 5). A four-point probe test was performed using one probe as a source, one probe as a ground, and two probes as intermediate measurements. This method was used because it does not require precise positioning of the probes to have replicable results. The program ramps the current in the source probe and calculates the resistance through the material from the voltage drop across the material. Current set points were chosen until the same resistance is calculated at all the current steps.

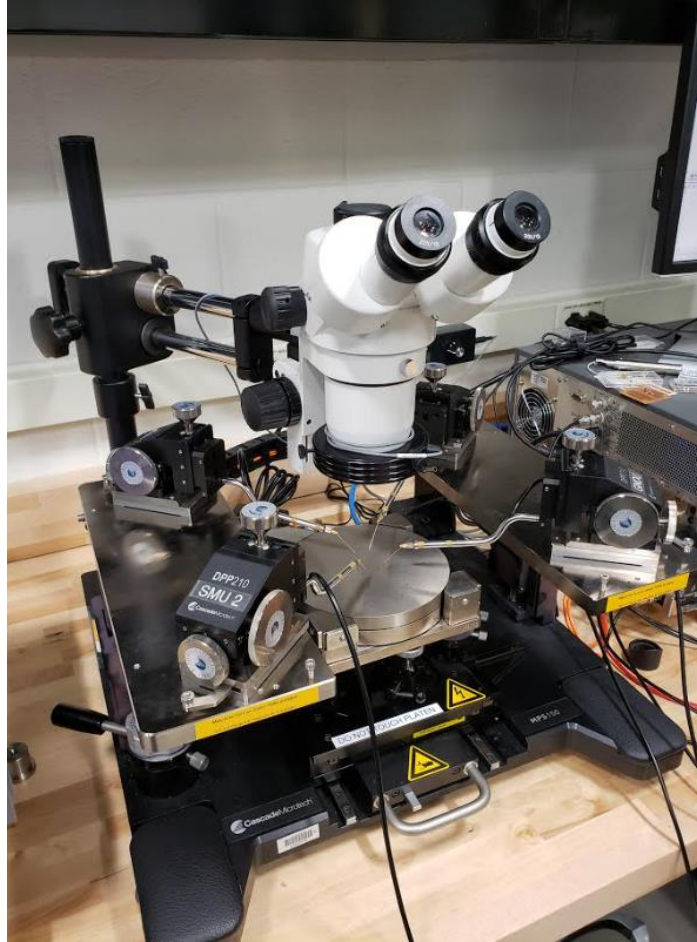


Figure 5: Traditional Electrical Probing Station

The above characterization methods appear to have worked well for both Mo and Re, but the W films could not have the thickness measured on the AFM. An alternative method, electron probe microanalysis (EPMA), is being explored by collaborators at the Air Force Research Lab, AFRL, to measure the thickness of the metal films. Mo EPMA results will be compared to AFM results to determine if thickness estimation for W can be performed using EPMA.

Conversion of Transition Metal Films to TMDs

After the transition metal films were deposited and characterized, the films were sent to collaborators in AFRL and Rice University to be converted to TMDs. The conversion was completed in a chemical vapor deposition (CVD) furnace. The metal films were heated to 550 °C, 650 °C, or 750 °C and exposed to excess vaporized sulfur/selenium. Raman spectroscopy was completed to determine if the metal films were converted to a crystalline TMDs. Raman spectroscopy displays peaks that indicate formation of the TMD compound, as well as its quality and crystalline nature. The refractive index and extinction coefficient of the TMDs was also used to indicate crystal quality.

Results and Discussion

The metal films were grown, and the thickness, roughness and conductivity were measured for each film. For the metal films the thickness was plotted compared to the conductance and roughness, as shown for room temperature Mo samples in Figure 6 and Figure 7, respectively.

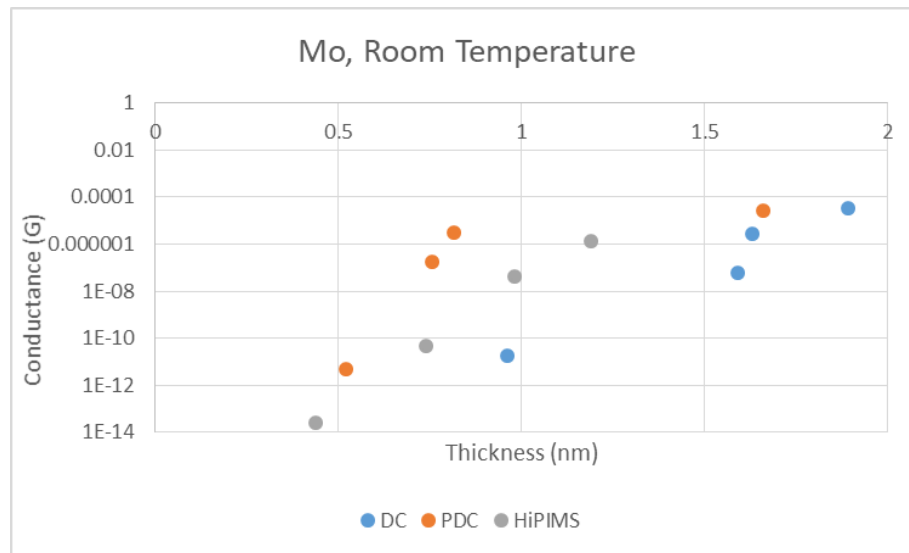


Figure 6: Thickness vs. Conductance of Room Temperature Mo Samples

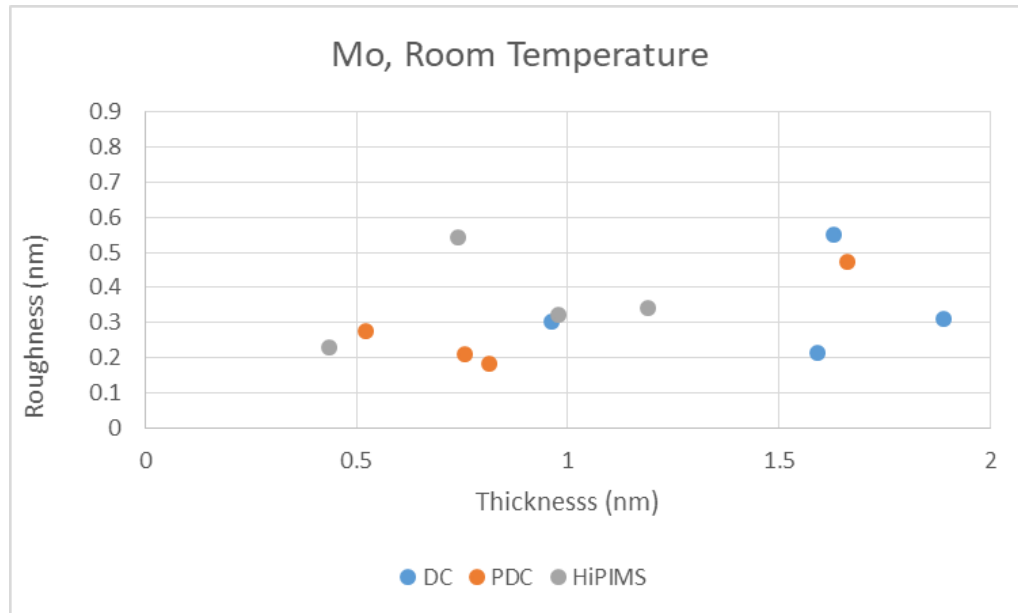


Figure 7: Thickness vs. Roughness of Room Temperature Mo Samples

Figure 6 highlights the effect power modulation has on the thickness that the metal film is continuous. The PDC films reach the continuity threshold with the thinnest layer of metal first, followed by HiPIMS and DC. As seen in Figure 7, power modulation does not have a large effect on the roughness of the material. The roughness did not follow a trend for any of the power supplies.

The thickness of the metal films was measured using the AFM. To have the best representation of the thickness of the metal films the largest possible scan width was used (50 μm). The thickness results for the shortest and longest deposition times for each power supply are shown for Mo in Figure 8. The thickness of the films increased with increased deposition time for each power supply. The lower the energy supplied by the power supply to the atoms was, the thicker the metal films were for a given deposition time. For reference, the thickness of an atom of Mo is 0.3nm. The thicknesses of the Mo films are not multiples of 0.3nm because the thickness is an average of the height difference over the entire scan.

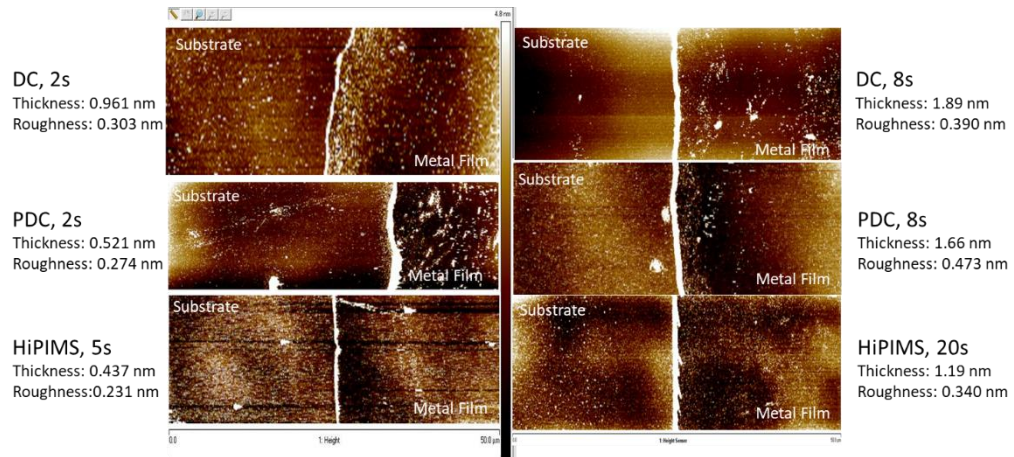


Figure 8: Thickness of Mo films

The roughness of the metal films was measured using the AFM. To best see the metal islands, a scan width of 500nm was selected through trial and error. The effect of deposition time and power supply on the crystal size is shown in Figure 9.

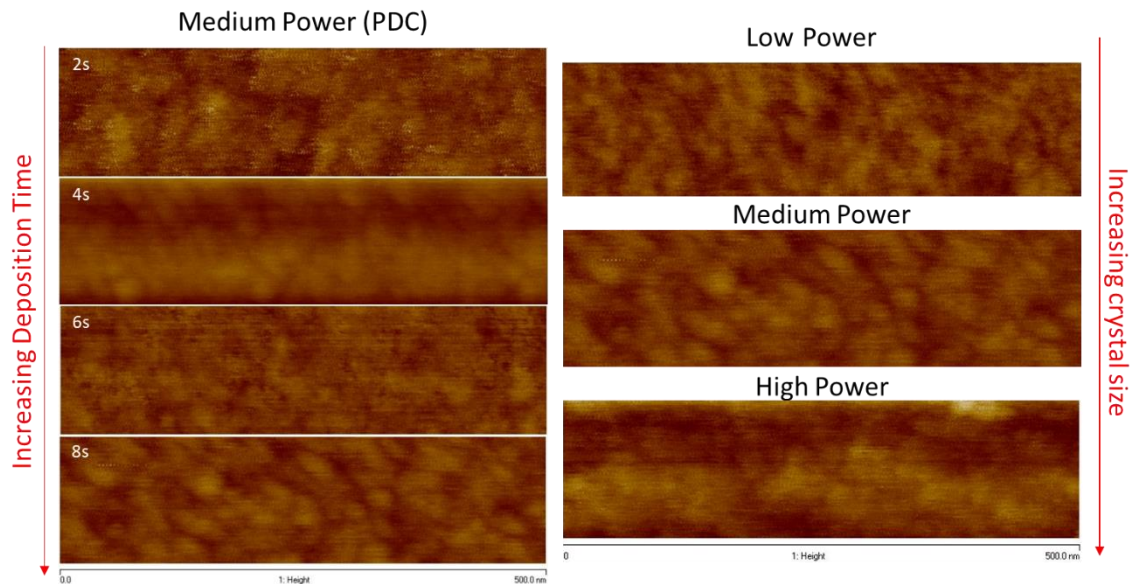


Figure 9: Deposition and Power Modulation Effect on the Roughness

For the same power supply, deposition time does not have an effect on the crystal size.

For the same deposition time, the crystal size increases with a higher energy power supply.

After the Mo films were exposed to Se by collaborators at AFRL and Rice University, Raman Spectroscopy was performed to confirm bond formation. The Raman shift plot, shown in Figure 10, displays the peaks of three different samples that were exposed to Se at different temperatures. All three samples were Mo deposited for 4 seconds with the PDC power supply.

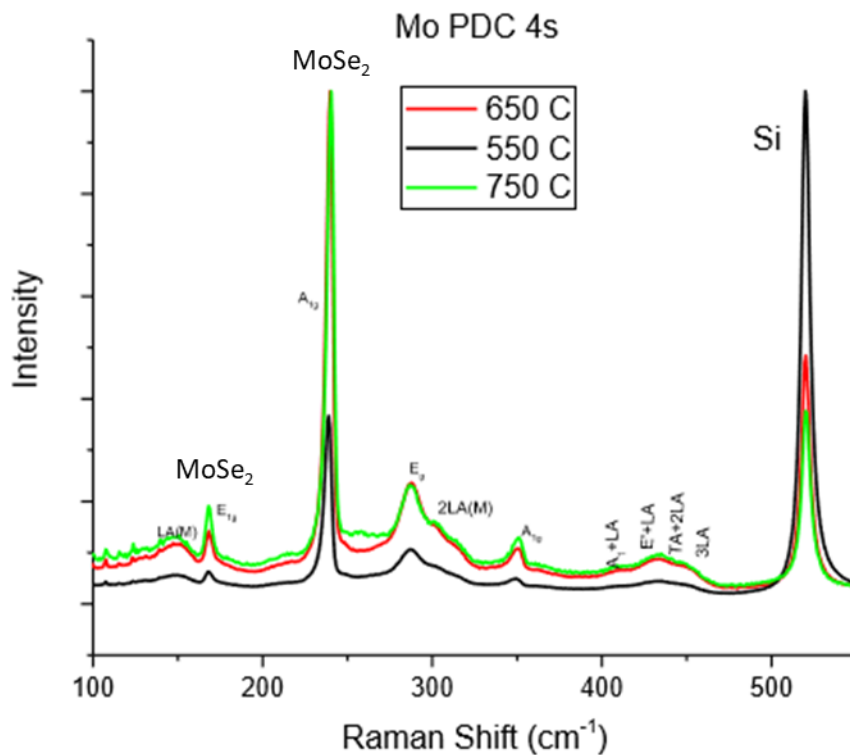


Figure 10: Raman Shift of Mo Samples Exposed to Se

The two peaks, A_{1G} and E_{1G} , were the expected peaks for in-plane and out-of-plane vibration of crystalline MoSe_2 , respectively. The Raman shift plot for amorphous materials, such as the metal films before they were exposed to the Se vapor, would be a flat line with no peaks. The additional peaks seen in Figure 10 are from other MoSe_2 peaks, as well as the SiO_2 substrate on which the metal films were deposited.

To see if the conversion of the metal films to the TMD was localized, the films were observed on an optical microscope. The films in Figure 11 show that the conversion was not localized, because the only differences in the film are impurities on the surface.

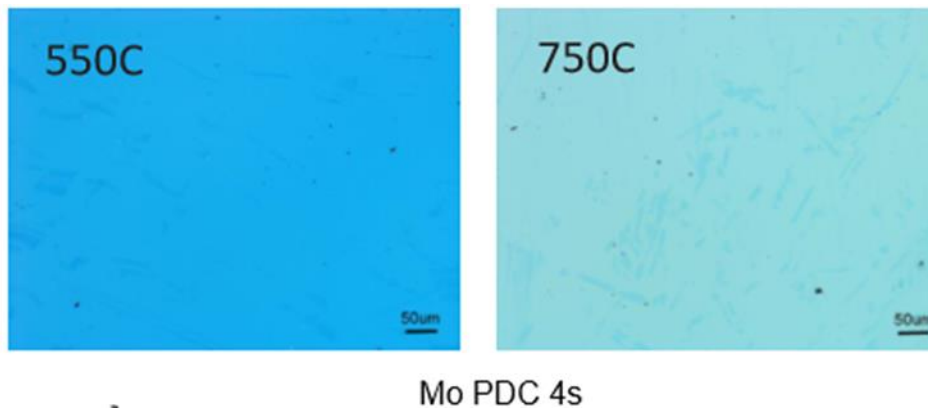


Figure 11: Optical Images of TMD Films.

The refractive index and extinction coefficient of selenized Mo films for different wavelengths of light was also measured to indicate the quality of the crystals formed (Figure 12).

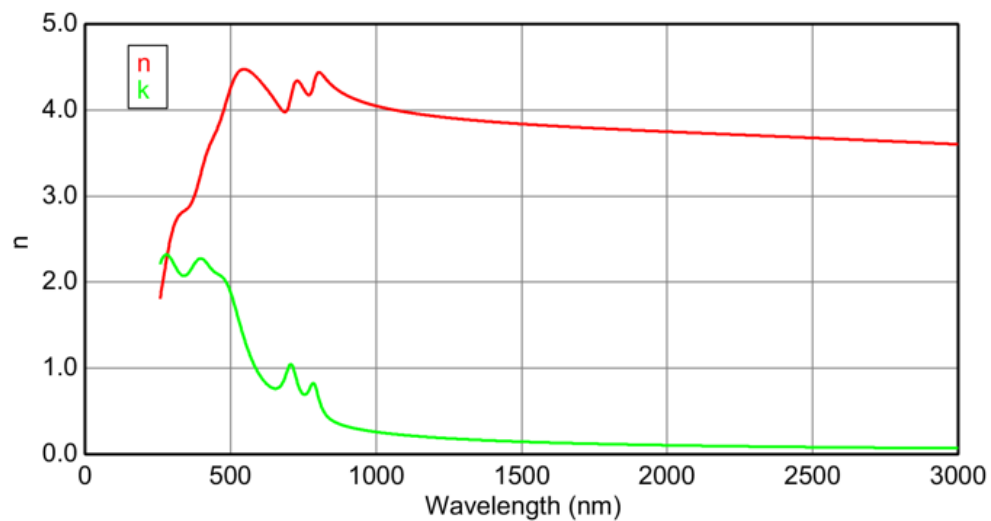


Figure 12: Refractive Index and Extinction Coefficient of Selenized Mo Films

The intensity and sharpness of the peaks between 500 and 1000 nm indicate crystal quality. The peaks are sharper for the selenized Mo films than what is seen in CVD films, indicating the potential for these new processes to make an impact on our ability to create large-scale, high quality 2D TMD materials.

Conclusion and Recommendations

Combining the results of the thickness, roughness, and conductivity, the Mo films with the most desirable characteristics had the conditions of 4 seconds deposition time, room temperature, with the PDC power supply (4s, PDC). 4s, PDC was selected because the sample was the thinnest film that was continuous and had little variation in height across the sample. When the 4s, PDC sample was exposed to Se vapor, conversion was successful. The higher the conversion temperature, the greater the peak intensity in the Raman shift graphs. The optical property data in Figure 12 indicate that there are less defects in the selenized Mo films than the state-of-the-art scalable CVD films. The diminished number of defects is likely due to the entire films being converted to a TMD instead of the localized conversion that is seen in CVD films.

For future experiments, PDC is the recommended power supply, unless another power supply or set of conditions is discovered that can produce a thinner continuous film. For future heterostructures and meshes, 4s, PDC will be the standard Mo layer used. The deposition time that produces a continuous film will likely differ depending on the material being deposited.

Future Work

The thicknesses of the W films need to be determined using EPMA or another method if EPMA is not reliable for these metal films. Combining the thickness of the W films with the conductivity data, the required thickness for film continuity can be determined. Understanding physical characteristics of the W films will allow for future heterostructure properties to be understood.

Superlattice heterostructures of Mo, W, and Re need to be made to determine how the stacking affects the characteristics of the material. First, superlattice heterostructures of Mo and W will be deposited to see how the order of material and the number of layers affects the properties of the material. Meshes of Mo and W will be deposited to determine how the material properties are affected when one layer contains two different metals. The superlattice heterostructures and meshes will be repeated twice with 1) Mo and Re, and 2) W and Re.

Once made and initial characterization completed, the superlattice heterostructure and mesh samples will be sent to collaborators at AFRL and Rice University to be converted to TMDs via exposure to gaseous sulfur/selenium. Then, the same characterization techniques will be used that confirmed the conversion and crystallinity of the MoSe₂ samples.

References

- Dumceno, D., Ovchinnikov, D., Lopez Sanchez, O., Gillet, P., Alexander, D. T., Lazar, S., . . . Kis, A. (2015). Large-area MoS₂ grown using H₂S as the sulphur source. *2D Materials*.
- Ehiasarian, A. P., New, R., Munz, W. -D., Hultman, L., Helmersson, U., & Kouznetsov, V. (2002). Influence of high power densities on the composition of pulsed magnetron plasmas. *Vacuum*, 147-154.
- Geim, A. K., & Grigorieva, I. V. (2013). Van der Waals heterostructures. *Nature*, 419-425.
- Jung, Y., Shen, J., Liu, Y., Woods, J. M., Sun, Y., & Cha, J. J. (2014). Metal Seed Layer Thickness-Induced Transition From Vertical to Horizontal Growth of MoS₂ and WS₂. *Nano Letters*, 6842-6849.
- Petrov, I., Barna, P. B., Hultman, L., & Greene, J. E. (2003). Microstructural evolution during film growth. *Journal of Vacuum Science & Technology A*, S117-S128.